JOURNAL OF SOLID STATE CHEMISTRY 24, 153–161 (1978)

Stability and The Equilibrium Selenium Vapor Pressure of the VSe_2 Phase

KOYA HAYASHI AND MITSUOKI NAKAHIRA

Okayama College of Science, Laboratory for Solid State Chemistry, 1-1, Ridai-cho, Okayama, 700, Japan

Received June 6, 1977; in revised form September 2, 1977

Determination of the homogeneity range of the VSe_2 phase was made. It extends from $V_{1.01}Se_2$ to $V_{1.18}Se_2$ at 800°C and from $V_{1.04}Se_2$ to $V_{1.10}Se_2$ at 300°C. The selenium-rich limit of the adjacent monoclinic phase is about $V_{1.20}Se_2$ between 700 and 1000°C. The two-phase region between monoclinic and the VSe_2 phases extends from $V_{1.18}Se_2$ to $V_{1.25}Se_2$ at lower temperatures. Above 700°C, the mixture of two phases becomes a pseudosingle phase of a mixed-layer type. Equilibrium vapor pressures of selenium on the solid V_xSe_2 ($x = 1.04$–1.28) were measured by a quartz Bourdon gauge between 600 and 1000°C. Activities and other partial molar quantities were evaluated. Stability of the vanadium atoms in the CdI_2-like V_xSe_2 phase was studied. A statistical model was applied for the nonstoichiometric V_xSe_2 with the CdI_2-like structure. Vanadium atoms in the vanadium-rich layers are more stabilized than those in the vanadium-poor layers, and the differences between each stabilizing energy was about 20.0 kcal/mole.

Introduction

In vanadium selenides, previous works are summarized in Table I. Røst and Gjertsen (*1*) found that the homogeneity range of the VSe_2 phase extended from $V_{1.18}Se_2$ to $V_{1.02}Se_2$ when quenched from 750°C. The two-phase region between the monoclinic and hexagonal CdI_2-like phases was not observed at 750°C. For slowly cooled samples, the two-phase region extended from $V_{1.11}Se_2$ to $V_{1.25}Se_2$ and the homogeneity range of the hexagonal VSe_2 phase was narrowed to an almost-line phase, $V_{1.11}Se_2$. Powder X-ray diffraction data of the $V_5Se_8(V_{1.25}Se_2)$ phase was also reported by Brunie and Chevreton (*5*).

Magnetic susceptibility of the VSe_2 phase was measured by Røst and Gjertsen (*1*) and recently be Van Bruggen and Haas (*8*) and also by Bayard and Sienko (*9*). Their results showed that only 2.3% V^{2+} was present as the interlayer vanadium and the rest as V^{3+}.

Throughout the above reports, no measurement was made regarding the selenium vapor pressure in equilibrium with the respective solid V_xSe_2. On the other hand, in cobalt and nickel selenides of NiAs-type structure, the equilibrium selenium vapor pressure was measured and the thermodynamic quantities were evaluated (*10*, *11*). A statistical model based on the assumption of random distribution of metal atoms and vacancies was applied for the nonstoichiometric NiAs-type structure. Vacancy formation energy and the interaction energy between the vacancies were estimated from the measured vapor pressure and that statistical model.

The scope of the present investigation is the determination of the homogeneity range of the VSe_2 phase, and the measurement of the equilibrium selenium vapor pressure of the solid VSe_2 phase, followed by the evaluation of the related thermodynamic quantities. Based on those measurements, a statistical model for the VSe_2 phase is also applied by assuming two different stabilization energies between the vanadium atoms in the vanadium-rich layer and those in the vanadium-poor layer. The

0022-4596/78/0242-0153 $02.00/0

TABLE I

COMPOUNDS OF VANADIUM–SELENIUM SYSTEM

Composition	Condition	Crystal	Lattice constants	Reference
V_5Se_4	750°C Quenched	Powder Tetragonal	$a = 9.294$ Å, $c = 3.417$ Å	(*1*)
VSe	1000°C Quenched	Powder Hexagonal	$a = 3.681$ Å, $c = 5.970$ Å	(*2*)
	750°C Slowly cooled	Powder Hexagonal	$a = 3.697$ Å, $c = 5.990$ Å	(*2*)
$V_{29}Se_{32}$	800°C Slowly cooled	Powder Hexagonal	$a = 7.211$ Å, $c = 24.002$ Å	(*2*)
V_7Se_8	900°C Slowly cooled	Powder Monoclinic	$a = 12.978$ Å, $b = 7.152$ Å $c = 23.978$ Å, $\beta = 90.40°$	(*3*)
V_3Se_4	Chemical Transport	Single Monoclinic	$a = 6.212$ Å, $b = 3.45$ Å $c = 11.88$ Å, $\beta = 91.5°$	(*4*, *7*)
$VSe_{1.5}$	750°C Quenched	Powder Monoclinic	$a = 6.123$ Å, $\beta = 3.440$ Å $c = 11.838$ Å, $\beta = 91.26°$	(*1*)
V_5Se_8		Powder Monoclinic	$a = 11.86$ Å, $b = 6.96$ Å $c = 17.74$ Å, $\beta = 91.21°$	(*5*)
VSe_2		Powder Hexagonal	$a = 3.34$ Å, $c = 6.12$ Å	(*6*)

stability of the vanadium atoms of non-stoichiometric V_xSe_2 phase is thus deduced according to that model.

Experimental

1. Phase relations. The starting materials were 99.999% pure selenium shot (Ishizu Pharmaceutical Co., Ltd.) and 99.9% pure vanadium powder (High Purity Chemicals Co., Ltd.). The vanadium and selenium were weighed, mixed, and put into a silica tube. The tube was evacuated (about 10^{-3} Torr) for 1 hr. Then it was sealed and preheated in a furnace (regulated within ±5°C by a high–low controller) at 500°C for 1 day. The specimen thus obtained was heated again 800°C for 1 day and kept at a fixed temperature (500 or 300°C) for 1 week for the low-temperature series. Since the specimen is heated at 800°C for 1 day for the completion of the reaction, it is at least almost equilibrated even at 300°C by holding it for 1 week. In fact, when a quenched speciment of apparent single phase at 800°C exhibited a phase separation at 300°C, 1 week holding was sufficient to complete the separation. For the high-temperature series, it was heated at 800°C for several days and quenched to room temperature. To find the composition, the content of vanadium was determined by completely oxidizing the specimen to V_2O_5 at 450–500°C in air. Some ignited specimens, V_2O_5, were analyzed for vanadium by the EDTA titration, resulting in around $V_2O_{5.02}$. This indicates that SeO_2 is negligible, if any, in the ignited specimen and the error in the composition, V_xSe_2, is within ±0.1 at.%.

The phases of vanadium selenides as analyzed by the ignition method were identified by the X-ray powder diffractometry of the Ni-filtered Cu$K\alpha$ radiation at room temperature. The reflection angles were corrected by the internal standard silicon. The lattice constants were calculated by the least-squares method using eight to ten sharp reflections.

2. Vapor pressure measurement. The vapor

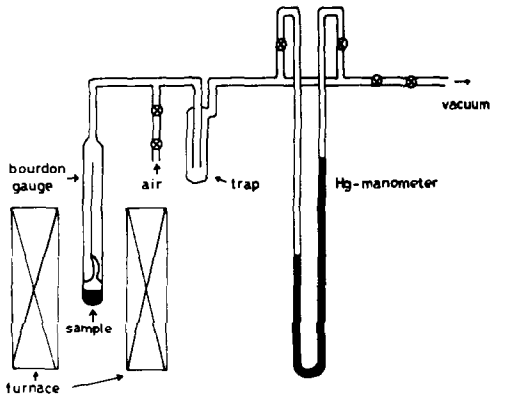

FIG. 1. Silica Bourdon gauge arrangement for measurement of selenium vapor pressures on V_xSe_2.

pressure was measured by a quartz Bourdon gauge. The construction of the apparatus is shown in Fig. 1. The Bourdon tube was baked under vacuum (about 10^{-3} Torr) at 1000°C for 1 hr. After that process, 3 g of the sample were put into the bottom of the Bourdon tube. Then it was evacuated (about 10^{-5} Torr) again for several hours at 100°C. After those processes, the sample part of the Bourdon tube was sealed. The space volume of the sample part was about 12 cm^3 (the change of the composition by evolution of the selenium vapor from the sample upon heating was calculated to be within 0.2 at.%). The measurement of the selenium vapor pressure was started from 500°C after heating at that temperature for 12 hr. The temperature of the sample was raised in 10–20°C steps and kept at the respective temperature for several hours within the low-temperature range (adjacent to 500°C) and for 10–30 min in the high-temperature range. The sensitivity of the Bourdon gauge was within 5 mm Hg.

Results and Discussion

1. Phase relations. The determination of the phase boundaries of the VSe_2 phase was made based on the identification of powder X-ray pattern, the measurement of the hexagonal lattice constants of the quenched specimens,

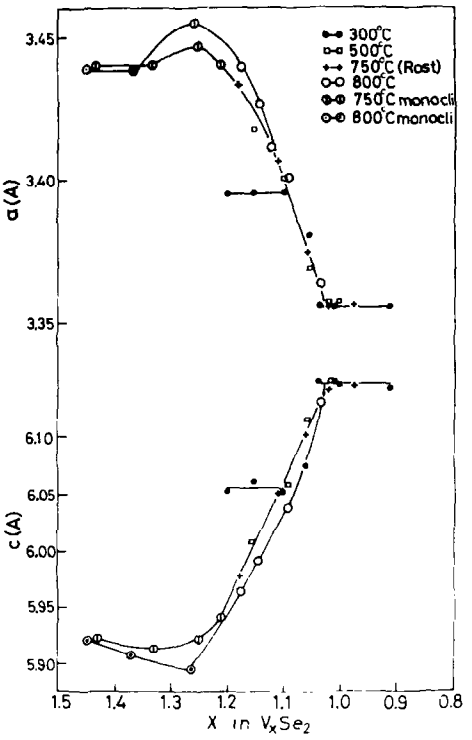

FIG. 2. Lattice constants of V_xSe_2 with a hexagonal cell.

and the measurement of the selenium vapor pressures. Determination of the selenium-rich boundary for the VSe_2 phase, and the two-phase region between the VSe_2 and monoclinic phases at 300°C were made by the measurement of the hexagonal lattice constants for the quenched samples shown in Fig. 2. In the figure the horizontal lines indicate the two-phase regions. The higher the sample temperature was, the more moved the selenium-rich boundary to the selenium-richer side. It was changed to $V_{1.01}Se_2$ at 800°C, $V_{1.03}Se_2$ at 500°C, and $V_{1.04}Se_2$ at 300°C. In comparison, Røst and Gjertsen (*1*) obtained $V_{1.02}Se_2$ for that boundary at 700°C.

Regarding the two-phase region, particular reference should be made here. The vanadium-rich boundary of the VSe_2 phase at 300°C was $V_{1.10}Se_2$ and the two-phase region was clearly observed. On the other hand, as can be seen from the figure, the lattice constants of the VSe_2 phase changed along a smooth curve to

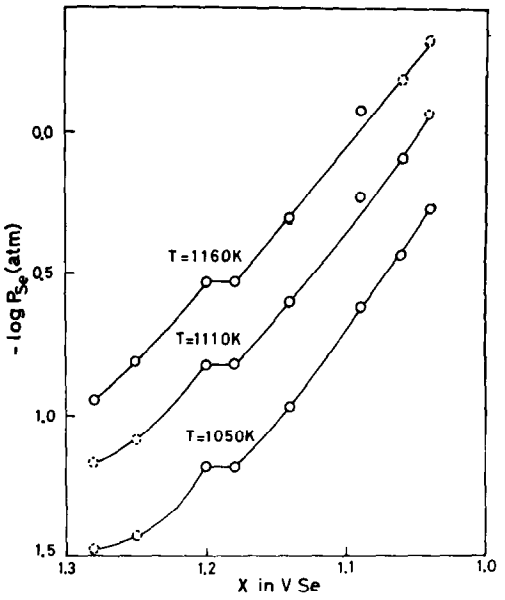

FIG. 3. Composition dependence of equilibrium selenium vapor pressures on V_xSe_2 ($x = 1.04$–1.28). The dotted circles represent the extrapolated values.

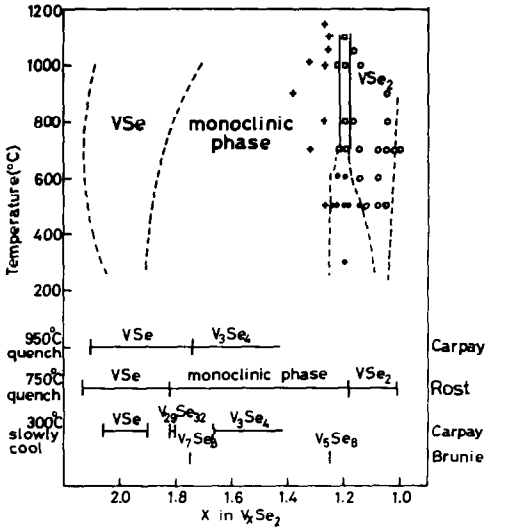

FIG. 4. Part of the phase diagram for vanadium–selenium system. The dashed line represents the boundary obtained by quenching method and the solid line by *in situ* method. Dashed circles represent VSe_2; solid circles, two phases between monoclinic and VSe_2, cross-line monoclinic phase and square mixed-layer phase.

the monoclinic phase and the two-phase region was not distinguished. However, according to the results of the equilibrium selenium vapor pressure measurements, the two-phase region was clearly distinguished even above 700°C (shown in Fig. 3). It was extended from $V_{1.18}Se_2$ to $V_{1.20}Se_2$ above 700°C. Of significance in the above two-phase region is that the powder X-ray pattern was very similar to that of the hexagonal VSe_2 phase. In addition to the broadness, however, of the reflections as compared with the sharpness of those of the hexagonal VSe_2 phase within that temperature range, a few reflections which did not belong to the monoclinic phase were mixed in the hexagonal pattern. (Those weak reflections were not used in the calculation of the hexagonal lattice constants.) The observations may reflect a formation of a mixed-layer lattice, and the region is tentatively regarded as of a pseudosingle mixed-layer one.

The other boundary was determined by the identification of the powder X-ray patterns of the quenched specimens. The vanadium-rich limit of the two-phase region between the monoclinic and hexagonal phases was $V_{1.24}Se_2$ at 500°C. Part of the phase diagram for the vanadium–selenium system is shown in Fig. 4. The phase diagram was made from both the present work and the results of previous works described in the introduction of the paper. In the diagram, the boundary obtained by an *in situ* vapor pressure measurement is represented as continuous line and the one by the quenching method as dashed line.

2. Equilibrium selenium vapor pressure measurement and the evaluation of some thermodynamic qualities. Selenium vapor pressures in equilibrium with the solid selenides are shown in Fig. 5. The sample Nos. 1 through 4 belong to the VSe_2 phase and the others to either the monoclinic or the mixture range. A few remarks should be made here regarding the selenium vapor. Many molecular species exist in the selenium vapor. The vapor pressure of selenium has been measured by Rau (*12*). According to his result, the molecular species in the selenium vapor are Se_2, Se_3, Se_4, Se_5, Se_6, Se_7, and Se_8. In the

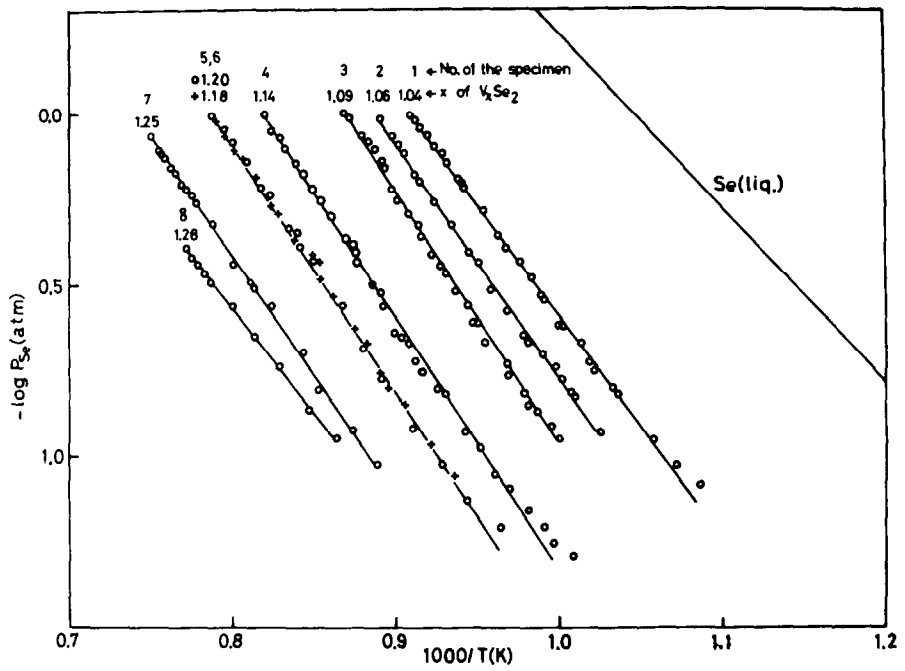

FIG. 5. Equilibrium selenium vapor pressures of V_xSe_2 versus reciprocal temperature.

following, the species Se_2 is taken as the reference species of activity calculations. The activity of the selenium vapor, a_{Se}, can be represented by the following equation.

$$a_{Se} = (P_{Se_2}/P^0_{Se_2})^{1/2}. \quad (1)$$

where P_{Se_2} is calculated from the measured total selenium vapor pressure, taking into account the dissociation and association of all the molecular species, Se_x ($x = 1$ through 8), at the respective temperature. The measured selenium vapor pressure is the sum of the partial pressures of all molecular species,

$$P_{\text{measured}}[\text{atm}] = \sum_{1}^{8} P_{Se_x}. \quad (2)$$

In that case, the following equation is held between the partial pressure P_{Se_x} and P_{Se_2} in equilibrium,

$$(P_{Se_2})^{x/2}/P_{Se_x} = K_x, \quad (3)$$

where K_x is the equilibrium constant. From "Eqs. (2) and (3)," the pressure of the reference species Se_2 is calculated. The K_x values were taken from the data of Mills (*13*). The saturated vapor pressure, $P^0_{Se_2}$, was also calculated according to the same procedure as the P_{Se_2} calculation from the data of Mills (*13*).

From those calculations, it was apparent that, around 870°K, the measured total pressure could be regarded as of P_{Se_2}, but with increasing temperature some correction within 0.15 in terms of the activity was needed. Therefore, in the following Figs. 6, 8, and 9 where $\log(a_{Se})$ is summarized, those corrected values were used. In Fig. 6, the activities, $\log(a_{Se})$, are plotted against the reciprocal specimen temperature. From the activities, partial molar enthalpies are calculated according to the following equation.

$$\log a_{Se}[\text{at } T_2] - \log a_{Se}[\text{at } T_1] = (\Delta\bar{H}_{Se}/2.303R)(1/T_2 - 1/T_2). \quad (4)$$

Also, the partial molar free energies are calculated according to the following equation,

$$\Delta G_{Se} = 2.30RT\log(a_{Se}). \quad (5)$$

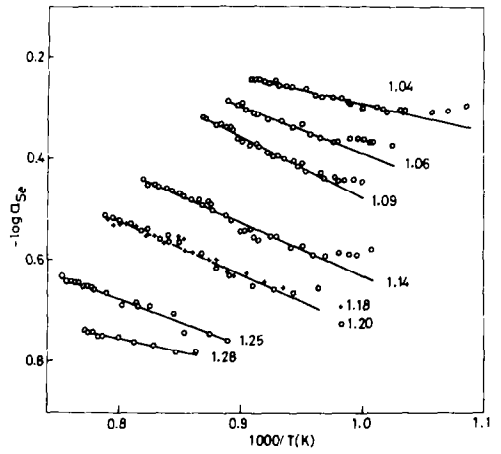

FIG. 6. Temperature dependence of activities of selenium of V_xSe_2 (x = 1.04–1.28). The number following each line represents the x value in V_xSe_2.

Those partial molar quantities of the VSe_2 phase are listed in Table II, in which the temperature ranges are also included.

3. Stability of the vanadium atoms in the VSe_2 phase. A schematic diagram for the crystal structure of the VSe_2 phase is shown in Fig. 7. In the VSe_2 phase, excess vanadium atoms from the stoichiometric composition are located in the interlayer position B which is sandwiched between the selenium layers. From the measurement of density and lattice constants, Røst and Gjertsen (*1*) have suggested a layer-type structure of this sort and the formation of selenium vacancies scarcely occurs. Therefore, the vanadium atoms can occupy the two different sites, A and B, in the structure.

In the figure, three different modes of the occupancy of vanadium atoms are possible. Mode I shows the structure in which the two vanadium site are equally occupied by the vanadium atoms. That is the case where no difference in the stabilization energy exists between the A- and B-sites. However, the tendency that excess vanadium atoms prefer the B-site strongly suggests that the vanadium atoms in the structure are stabilized with different energies between the A- and B-sites. Modes II and III represent such cases. Mode II shows an arrangement in which the A-sites are fully occupied with the B-sites being partially filled. That is the special case of Mode III in which the A-sites are nearly occupied and the B-sites are partially filled. Mode I with the equivalent A- and B-sites is of the defective NiAs-type, while Modes II and III are of the CdI_2-type. In the present work, therefore, a statistical model is considered according to the Modes II and III. Moreover, since the Mode III represents a general case, the following statistical calculations were carried out for only the Mode III.

(a) Vanadium-rich site is called A-site and the poor-one B-site. Stabilization energy for the

TABLE II

PARTIAL MOLAR QUANTITIES OF V_xSe_2 PHASES[a]

Composition	$-\Delta\bar{H}_{Se}$ (kcal/mole)	$-\Delta\bar{G}_{Se}$ (kcal/mole)		
X	(°K)	1000°K	1050°K	1100°K
1.04	2.3_6 (920–1100)	1.3_5	1.2_8	1.2_3
1.06	4.3_2 (980–1125)	1.7_9	1.6_6	1.5_4
1.09	5.5_8 (1000–1150)	2.2_0	2.0_2	1.8_5
1.14	4.8_8 (990–1220)	2.9_0	2.8_0	2.7_0
1.18	4.8_3 (1070–1265)	(3.3_6)	3.2_9	3.2_2
1.20	4.8_3 (1040–1270)	(3.3_6)	3.2_9	3.2_2
1.25	4.1_2 (1100–1320)	(3.9_1)	(3.9_0)	(3.8_9)
1.28	2.4_1 (1160–1300)	(3.9_3)	(4.0_1)	(4.0_9)

[a] ( ) Extrapolated values.

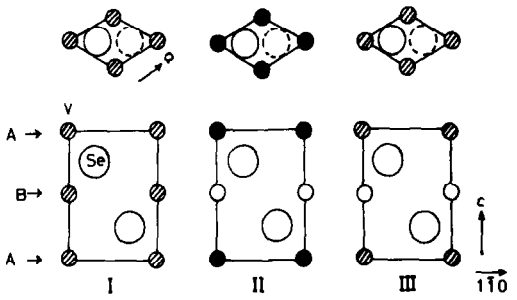

FIG. 7. Schematical diagrams for crystal structure of the VSe_2 phase. Modes of the site occupation by vanadium atoms; the large circles represent the selenium site; small open circles, the partially filled vanadium sites; small solid circles, the perfectly filled vanadium sites; and hatched circles, the almost-filled vanadium sites.

vanadium atom in the A-site is defined E_A and for that of the B-site, E_B.

(b) In the high-temperature range, it is thought that the vanadium atoms and vacancies are randomly distributed within each layer—*interlayer* disordering.

(c) The number of the total metal sites equals the number of the selenium atoms. The number of the A-sites equals half of the total metal sites and the number of the B-sites also half of that.

(d) Regarding the entropy, only the configurational entropy is considered and the others are regarded as the simple summation of the entropies of the pure components.

(e) Each quantity is represented with the following notation:

M total number of selenium atoms,
N total number of vanadium atoms,
n_A number of vanadium atoms on the A-site,
n_B number of vanadium atoms on the B-site.

By using the notations described above, the partition function and the free energy are written as follows,

$$\Gamma = \sum \frac{[(M/2)!]^2 \exp[-(n_A E_A + n_B E_B)/RT]}{n_A! n_B! (M/2 - n_A)! (M/2 - n_B)!} \cdot \Gamma^0 \tag{6}$$

and

$$\Delta G = n_A E_A + n_A E_A - RT[M \ln(M/2) - n_A \ln(n_A) - n_B \ln(n_B) - (M/2 - n_A)\ln(M/2 - n_B) - (M/2 - n_B)\ln(M/2 - n_B)] + \Delta G^0. \tag{7}$$

Γ^0 and ΔG^0 and respectively the partition function and the free energy for the mixture of the pure components, vanadium and selenium. As can easily be recognized through the Modes II and III in Fig. 7, the occupancy of the A-site, n_A, indicates the degree of interlayer disordering.

At the equilibrium state, ΔG gets to the minimum and, since $n_A + n_B = N$, "Eq. (7)" can be differentiated with respect to n_A, giving the value of n_A at the equilibrium state, $(d\Delta G/dn_A)_{T,N,M} = 0$. The result is the following equation,

$$n_A = \frac{(M/2 + N + PM/2 - PN) - ((M/2 + N + PM/2 - PN)^2 - 2MN(1 - P))^{1/2}}{2(1 - P)}, \tag{8}$$

where $P = \exp[(E_A - E_B)/RT]$. And the chemical potential of selenium is calculated as follows,

$$\mu_{Se} = (E_A - E_B)N' - RT[\ln(M/2) - N'(\ln n_A - \ln(N - n_A)) - (1/2 - N')\ln(M/2 - n_A) - (1/2 + N')\ln(M/2 + n_A - N)] + \mu^0_{Se}, \tag{9}$$

where $N' = (1 + P)/4(1 - P) - [M(1 + P)^2/2 - N(1 - P)^2]/4(1 - P)[(M/2 + N + PM/2 - PN)^2 - 2MN(1 - P)]^{1/2}$.

At equilibrium, the chemical potential of selenium in the solid phase should be equal to that of the vapor phase, and therefore the activity can be expressed in the following equation in terms of the selenium activity, a_{Se}, as measured by the Bourdon gauge.

$$\ln(a_{Se}) = (\mu_{Se} - \mu^0_{Se})/RT. \tag{10}$$

Experimental values of activities, a_{Se}, versus the composition of the VSe_2 phase are shown in Fig. 8.

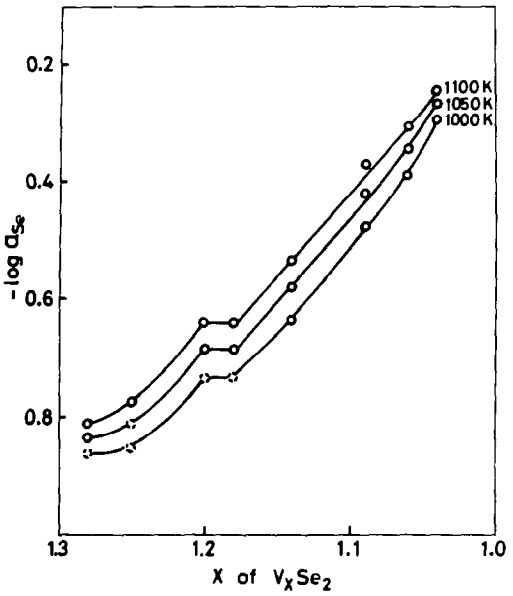

FIG. 8. Composition dependence of activities of selenium of V_xSe_2 (x = 1.04–1.28). The dashed circles represent the extrapolated values.

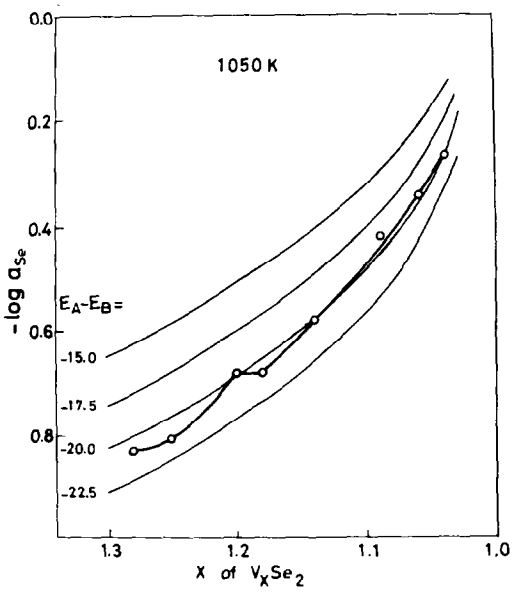

FIG. 9. Calculated values of activities of selenium for the VSe_2 phase. The open circles represent the experimental values and the other thin lines represent the calculated values.

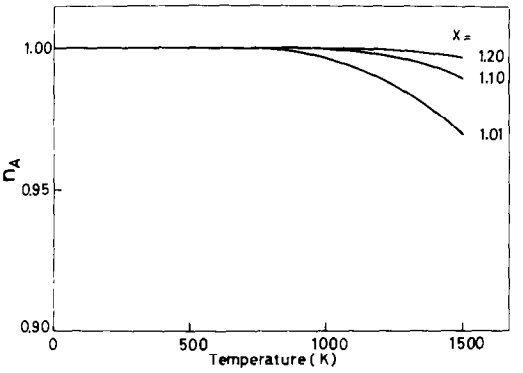

FIG. 10. Occupation ratio of the interlayer vanadium-rich site by vanadium atoms. Calculated from Eq. (8) in the text. The value x represents the composition of V_xSe_2.

Through careful inspections of "Eqs. (8), (9), and (10)" which give the number of vanadium atoms in the A-site of the stabilized solid, one can easily see that only $(E_A - E_B)$ is involved in the activity as the energy term. This leads to a conclusion that, as far as the energy is concerned, the activity is a function of only the energy difference, $(E_A - E_B)$. Upon assuming the energy difference, $(E_A - E_B)$, being -15.0, -17.5, -20.0, or -22.5 kcal/mole, respectively, a computer (Melcom 7700) calculation was made of the relation between the activity and the composition. The results are shown in Fig. 9. In the figure, in order to obtain the best fit with the experimental values, 1.139 was added to each calculation. This is because a correction should be made corresponding to the heat of fusion of selenium in the solid compounds, since the calculations were based on the liquid selenium as the standard state. As evident from the figure, the best fit with the experimental values involves the energy difference, $E_A - E_B$, being -20.0 kcal/mole. By using this value, the occupation ratio of the A-site was calculated according to "Eq. (8)" and the results are shown in Fig. 10. From the figure, one can see that at low temperatures the A-site is nearly fully occupied. With increasing temperature, part of the A-site atoms tends to move to the B-site (interlayer disordering). However, within the

present experimental range (up to about 1300°K), the *interlayer* disordering scarcely occurs. Similar observation was made of V_5S_8 by Nakazawa *et al.* (*14*) in which the interlayer disordering was only about 50% at the *intralayer* order–disorder transition at about 800°C, and further disordering did not take place until the maximum experimental temperature, 1000°C.

Summary

Within the present experimental temperatures, interlayer disordering of the vanadium atoms and vacancies scarcely takes place, and the vanadium atoms in the A-site are 20.0 kcal/mole more stabilized than those in the B-site. The energy difference is thought to be caused by the difference in the selenium–vanadium bonding energy at each A- and B-site.

In the present consideration, E_A and E_B are considered constant regardless of the changes in the temperature and composition. Judging from the change in the lattice constant, that may not be necessarily true, but as far as the present experimental range is concerned, $E_A - E_B$ is approximately constant as suggested by the inspection of Figs. 9 and 10.

The lattice expansion by an *in situ* X-ray experiment which showed the importance of selenium–vanadium bonding as well as theoretical calculations of E_A and E_B will be reported in the near future. In addition, the ordered structures at low temperatures will also be reported.

Acknowledgment

The authors' thanks are due to the Ministry of Education for its grant-in-aid by which part of the present work was made possible.

References

1. E. RØST AND L. GJERTSEN, *Z. Anorg. Allg. Chem.* **328**, 299 (1964).
2. F. M. A. CARPAY, *J. Inorg. Nucl. Chem.* **28**, 2827 (1966).
3. S. BRUNIE, M. CHEVRETON, AND J-M. KAUFFMANN, *Mater. Res. Bull.* **7**, 253 (1972).
4. F. M. A. CARPAY, *Philips Res. Rep. Suppl.* 10 (1964).
5. S. BRUNIE AND M. CHEVRETON, *C.R. Acad. Sci. Paris* **258**, 5847 (1964).
6. E. HOSCHEK AND W. KLEMM, *Z. Anorg. Allg. Chem.* **242**, 53 (1939).
7. F. BERTAUT AND M. CHEVRETON, *C.R. Acad. Sci. Paris* **255**, 1275 (1962).
8. C. F. VAN BRUGGEN AND C. HAAS, private communication.
9. M. BAYARD AND M. J. SIENKO, *J. Solid State Chem.* **19**, 325 (1976).
10. H. JELINEK AND K. K. KOMAREK, *Monatsh. Chem.* **105**, 689 (1974).
11. H. JELINEK AND K. L. KOMAREK, *Monatsh. Chem.* **105**, 917 (1974).
12. H. RAU, *Ber. Bunsenges. Phys. Chem.* **71**, 711 (1967).
13. K. C. MILLS, "Thermodynamic Data for Inorganic Sulphides, Selenides and Tellurides," pp. 80–84, 85–93, Butterworths, London (1974).
14. H. NAKAZAWA, M. SAEKI, AND M. NAKAHIRA, *J. Less-Common Metals* **40**, 57 (1975).